Trapped surfaces in nonspherical initial data sets and the hoop conjecture

Eanna Flanagan
Theoretical Astrophysics, California Institute of Technology, Pasadena, California 91125
(Received 8 April 1992)

The existence of outer trapped surfaces in conformally flat, axisymmetric, momentarily static initial data sets for Einstein's equations is investigated. It is shown that none of the level surfaces of the conformal factor can be outer trapped, whenever the minimum value of the circumferences (or of the square roots of the areas) of all the surfaces surrounding the source region is greater than a constant times the Arnowitt-Deser-Misner mass. This result is along the lines of the hoop conjecture. It also provides evidence in favor of the conclusion of Shapiro and Teukolsky, drawn from recent numerical relativity calculations, that the gravitational field on a spacelike hypersurface can become arbitrarily singular without the appearance of an apparent horizon.

PACS number(s): 04.20.Cv, 02.40.+m, 97.10.Nf, and 97.60.Lf

I. INTRODUCTION AND SUMMARY

The concept of a closed trapped surface (CTS) has been a crucial tool in furthering our understanding of gravitational collapse. Thanks to the celebrated singularity theorems of Hawking and Penrose [1] we know that if locally measured energy densities are positive, then the appearance of a CTS signifies that a point of no return has been passed: classical general relativity dictates that a singularity must form, independently of the equation of state of the collapsing matter. If one assumes that cosmic censorship is true, then the existence of a CTS also implies that an event horizon is present [2]. Even in the absence of this assumption, Israel [3] has established a gravitational confinement theorem which roughly states that "if a closed trapped surface forms, it can be extended into a spacelike three-cylinder on which the future directed light cones are always inward pointing." This suggests that the singularity which is formed is non-naked.

Thus there is considerable motivation for finding necessary and sufficient conditions for the formation of CTS's. Such conditions would justify and make precise the popular belief that if enough matter is compacted into a small enough region then a black hole must be formed. Many efforts have been made in this direction [4–7]. Simple dimensional considerations tell us that a suitable sufficient condition is that $m \lesssim \ell$, where m is a typical mass scale and ℓ is a typical length scale of the collapsing configuration. (We set Newton's gravitational constant and the speed of light to unity.) Attempts to make this condition more precise must face up to the following problem: in extreme, strong field situations, the masses and lengths that are measured by internal and by external observers may differ by large factors. Specifically, for an isolated collapsing body the Arnowitt-Deser-Misner (ADM) mass [8] may be small compared to the total proper mass [9], and internally measured radii may be large compared to surface measures of size [10]. So which mass and length are appropriate for a criterion of the type $m/\ell \lesssim 1$?

For spherically symmetric spacetimes, which are relatively well understood, these questions have been resolved [11]. Let m_p denote the total proper mass inside a spherical surface S, and m_H the Hawking mass of S, which coincides with the ADM mass when the exterior to S is vacuum. Let r_p denote the proper radius of the sphere and r_S the Schwarzschild radius, so that $4\pi r_S^2$ is the area. Then sufficient conditions for the existence of CTS's are [12] (i) $m_p/r_p > 1$ and (ii) $m_H/r_S > \frac{1}{2}$, while necessary conditions for S to be outer trapped are (i) $m_p/r_p > \frac{1}{2}$, (ii) $m_p/r_S > 1$, and (iii) $m_H/r_S > \frac{1}{2}$.

Strongly aspherical spacetimes are less well understood. For criteria involving internally measurable quantities, Schoen and Yau have proved a very general sufficient condition for the existence of CTC's of the form (minimum density) $\times$ (radius squared) $\geq$ const [6]. In terms of externally measurable quantities, there is some evidence in favor of Thorne's (1972) hoop conjecture (HC): *Black holes with horizons form when and only when a mass M gets compacted into a region whose circumference in every direction is $\mathcal{C} \lesssim 4\pi M$* [13–15].

Recent numerical relativity calculations of gravitational collapse by Shapiro and Teukolsky [16] provide strong evidence in favor of the HC. For collapsing prolate and oblate spheroids, apparent horizons (marginally outer trapped surfaces) appear in a particular time slice as soon as the condition $\mathcal{C}_{\min} \lesssim 4\pi m_\infty$ is satisfied. Here m_∞ is the ADM mass and $\mathcal{C}_{\min}$ is the minimum of the circumferences of axisymmetric surfaces surrounding the spheroid. The circumference of an axisymmetric surface S is defined as

$$\mathcal{C}(S) = \max(L_e, L_p), \tag{1.1}$$

where L_e is the maximum of the lengths of closed azimuthal curves, and L_p is twice the distance from the north pole to the south pole. For sufficiently elongated prolate spheroids which collapse down to a spindle, $\mathcal{C}_{\min} = L_p$ does not change appreciably during the collapse and so the HC predicts that no trapped surfaces should be formed. This is precisely what Shapiro and Teukolsky find, and they cite this and an apparent singularity at the spindle's end as evidence that cosmic censorship is violated. Analytic models by Barrabes, Israel and Letelier [18] of thin shells collapsing with the speed of light show qualitatively similar features to these numerically generated spacetimes and reinforce these conclusions.

The purpose of this paper is to investigate the occurrence of outer trapped surfaces in axisymmetric initial data sets, and to present a proof of the 'only when' part of the HC, interpreted in the sense described above, under some restrictive limitations and assumptions. Our approach is to try to find constraints that must be satisfied by quantities of the form $m(S)/r(S)$, when the surface S is, or is not, trapped. Here $m(S)$ is a measure of the mass inside S, and $r(S)$ is a measure of the size of S.

This work was in part inspired by a recent paper of Malec [19], where, using similar assumptions and a similar approach, he finds conditions for the existence of closed, outer-trapped surfaces in momentarily static, conformally flat initial data sets. Malec's conditions are expressed in terms of the internal quantities r_p (proper radius) and m_p (proper mass). In this paper, we focus instead on the following external quantities: the circumferential radius of a surface S,

$$r_c(S) \equiv \frac{\mathcal{C}}{2\pi} = \frac{1}{2\pi}\max(L_e, L_p), \tag{1.2}$$

the Schwarzschild radius $r_S(S)$ defined so that $4\pi r_S^2$ is the area of S (also considered by Malec), and the asymptotic ADM mass m_∞.

We restrict attention to asymptotically flat, axisymmetric initial value hypersurfaces, that are conformally flat and momentarily static outside a compact source region in which the matter density is nonvanishing. We need not assume anything about the interior of this source region. With these assumptions we can write the three-metric of the hypersurface in the external region in the form $h_{ab} = \Phi^4 \bar{h}_{ab}$, where the metric $\bar{h}_{ab}$ is flat, and Φ is a conformal factor. We also restrict attention to surfaces S which lie outside of and surround the source region.

The first of our two main conclusions is as follows.

Theorem 1. Let S be a level surface of the conformal factor Φ in the external region, and be convex with respect to $\bar{h}_{ab}$. Then

$$\frac{m_\infty}{r_c(S)} \leq \frac{\pi}{8}\sqrt{1+\frac{\pi^2}{4}} \approx 0.73. \tag{1.3}$$

An examination of various examples (see Appendix C) indicates that the least possible upper bound for the quantity m_∞/r_c is probably 1/2. Also in Appendix C we give an example of an initial data set which shows that no analogous upper bound applies to the quantity m_∞/r_S.

The physical interpretation of Theorem 1 is that if a body has passed a certain critical degree of compression (as measured by m_∞/r_c), then it cannot be momentarily static; i.e., it must be collapsing. A similar result of the form $m_p/r_p \leq$ const is established in Ref. [19], with roughly the same physical interpretation.

To motivate our second result, we briefly review the general behavior of our chosen type of initial data set. Because of time symmetry, there can be no trapped surfaces present, only outer trapped ones. If these are present, then in the spherically symmetric case the ratio $m_\infty/r_c = m_\infty/r_S$ varies with radius as shown in Fig. 1. We see that deep inside the trapped region the ratio can be arbitrarily small. This behavior persists in strongly aspherical initial data sets. In Sec. II B we show that if S is a convex, level surface of the conformal factor, then

$$\frac{m_\infty}{r_c} = f_1(\Phi_{|S}) f_2(S), \tag{1.4}$$

where the function f_2 is bounded above and $f_1(x) \equiv 4(x-1)/x^2$. Now if the source is sufficiently compact that just outside the source the conformal factor satisfies $\Phi \gg 1$, then we see from this equation that that the ratio m_∞/r_c will be $\ll 1$ there. The ratio will also be $\ll 1$, of course, at large distances from the source. Only in some intermediate region, where $\Phi \sim 2$, will it become of order unity. See Ref. [20] and also Appendix C for some examples.

Because of this behavior we cannot hope to establish a necessary condition of the form $m_\infty/r_c(S) \geq$ const for a surface S to be outer trapped. (This is in contrast with the situation in Ref. [19] where Malec does find such a condition for the ratio m_p/r_p.) However, a necessary condition which does work is that if S is outer trapped, then there must exist *some* surface S' outside S for which the ratio $m_\infty/r_c(S')$ is of order unity. This is essentially the interpretation of the HC for which Shapiro and Teukolsky find strong evidence [16], and which we shall make precise in our second theorem.

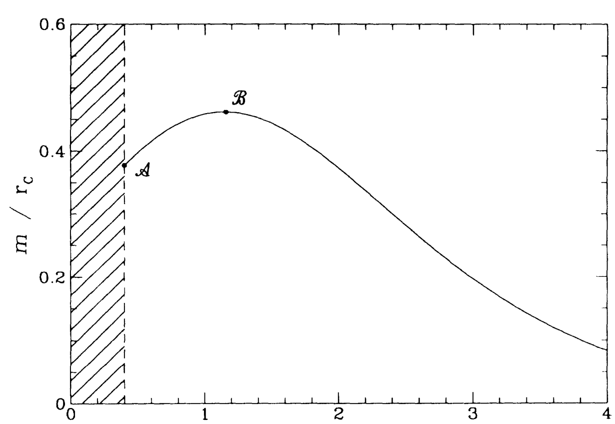

FIG. 1. The ratio m_∞/r_c as a function of some radial coordinate ξ outside the source region (shaded), in a typical momentarily static, conformally flat initial data set. The turnaround seems to always occur when there are outer trapped surfaces present, and these are then found in the region between points $\mathcal{A}$ and $\mathcal{B}$. For some other data sets, as one decreases ξ, the matter surface is reached before the ratio comes to a local maximum.

Our second theorem depends on a property [Eq. (2.38) below] of the foliation of the external region by level surfaces of the conformal factor. This property holds for a large class of foliations, and we conjecture that it is always satisfied.

Theorem 2. Suppose that all the level surfaces of Φ in the external, source free region are convex with respect to $\bar{h}_{ab}$ and satisfy Eq. (2.38), and that some level surface in the external region is outer trapped. Then there exists another level surface S' such that

$$\frac{m_\infty}{r_c(S')} \geq \frac{\pi}{4}\left(1-\frac{1}{\sqrt{2}}\right), \tag{1.5}$$

and

$$\frac{m_\infty}{r_S(S')} \geq 1-\frac{1}{\sqrt{2}}. \tag{1.6}$$

The above results are derived in Sec. II. Some technical details are relegated to Appendices A and B. In Appendix C we give an analysis of a class of initial data sets whose sources are ellipsoidal thin shells of matter, in order to motivate and illustrate the general results. Our notation and conventions follow those of Ref. [21].

II. AXISYMMETRIC, CONFORMALLY FLAT, MOMENTARILY STATIC INITIAL DATA SETS

A. Governing equations

In this section we write down the initial value equations and define the various measures of mass and radius that we use. An initial data set for Einstein's equations consists of a three-manifold Σ with a three-metric h_{ab}, extrinsic curvature tensor K_{ab}, matter density ρ_M, and momentum density j^a. These must satisfy the initial value equations [21]

$$^{(3)}R = \mathrm{tr}(K^2) - (\mathrm{tr}K)^2 + 16\pi\rho_M \tag{2.1}$$

and

$$D_a K^{ab} - D^b \mathrm{tr}\, K = 8\pi j^b, \tag{2.2}$$

where $^{(3)}R$ is the Ricci scalar and D^a the covariant derivative operator associated with the metric h_{ab}. If we specialize to maximal slices ($\mathrm{Tr}K = K_a{}^a = 0$), then these equations can be simplified by making a conformal transformation [22] to new variables $\bar{h}_{ab} = \Phi^{-4} h_{ab}$, $\bar{K}_{ab} = \Phi^2 K_{ab}$. This gives

$$\left[\bar{D}_a\bar{D}^a - \frac{1}{8}{}^{(3)}\bar{R}\right]\Phi = -\frac{1}{8}\Phi^{-7}\mathrm{tr}(\bar{K}^2) - 2\pi\rho_M\Phi^5, \tag{2.3}$$

and

$$\bar{D}_a\bar{K}^{ab} = 8\pi\Phi^{10} j^b. \tag{2.4}$$

Here $\bar{D}_a$ is the derivative operator associated with the unphysical metric $\bar{h}_{ab}$.

Consider now closed two-surfaces S of spherical topology in the slice Σ. If n^a is the unit outward normal to S, the expansions of the future directed, inward and outward directed, null geodesic congruences normal to S are

$$\theta_{\rm in} = -D_a n^a + (h_{ab} - n_a n_b)K^{ab} \tag{2.5}$$

and

$$\theta_{\rm out} = D_a n^a + (h_{ab} - n_a n_b)K^{ab}. \tag{2.6}$$

In terms of the conformally transformed metric $\bar{h}_{ab}$ and normal $\bar{n}^a$ (normalized by $\bar{h}_{ab}\bar{n}^a\bar{n}^b = 1$), we get

$$\theta_{\rm out,in} = \pm\Phi^{-2}\left[\bar{D}_a\bar{n}^a + 4\bar{n}^a\bar{D}_a \ln\Phi\right] - \Phi^{-6}\bar{K}_{ab}\bar{n}^a\bar{n}^b, \tag{2.7}$$

where the upper sign refers to the outwards expansion. The surface S will be trapped if $\theta_{\rm in} < 0$ and $\theta_{\rm out} < 0$ everywhere, and outer trapped if $\theta_{\rm out} < 0$. The property of being outer trapped is sufficient for the singularity theorems to hold [23], and to guarantee that an apparent horizon is present.

We now specialize to the following type of initial data set. Divide Σ into a compact interior region Σ_i and an exterior region Σ_e which has the topology of Euclidean three-space with a ball removed. Suppose that all the sources are contained in Σ_i, so that $\rho_M = j^a = 0$ in Σ_e, and that all the level surfaces of the coformal factor Φ in Σ_e have spherical topology [24]. Suppose also that the exterior region is axisymmetric, conformally flat and momentarily static, then $K_{ab} = 0$ and $\bar{h}_{ab}$ is flat in Σ_e [25]. The metric h_{ab} is given in cylindrical coordinates by

$$ds^2 = \Phi^4(\rho,z)(d\rho^2 + dz^2 + \rho^2 d\varphi^2), \tag{2.8}$$

where from Eq. (2.3) the conformal factor Φ satisfies Laplace's equation

$$\bar{D}_a\bar{D}^a\Phi = 0. \tag{2.9}$$

The measures of mass and of size that we will use are as follows. The ADM mass of Σ is given by [8]

$$m_\infty = -\frac{1}{2\pi}\oint_S \bar{n}^a\bar{D}_a\Phi \; d^2\bar{S}, \tag{2.10}$$

where S is any surface enclosing the source region Σ_i. The Schwarzschild radius of a surface S is defined by

$$4\pi r_S^2 = \mathcal{A}(S) = \oint_S \Phi^4 d^2\bar{S}, \tag{2.11}$$

where $\mathcal{A}(S)$ is the area of S. Let D be the curve where S intersects the half plane $\varphi = 0$. The circumferential radius is

$$r_c = C/2\pi = \frac{1}{2\pi}\max(L_e, L_p), \tag{2.12}$$

where the length of the longest closed azimuthal curve on S is

$$L_e = \sup_{x\in D}\; 2\pi\rho(x)\Phi(x)^2, \tag{2.13}$$

and twice the distance from the north pole to the south pole is

$$L_p = 2 \int_D \Phi^2 dl. \tag{2.14}$$

Note that it follows from these definitions that $r_S^2 = \frac{1}{2}\int_D \rho\Phi^4 dl \leq \left[\sup_{x\in D}\rho(x)\Phi(x)^2\right]\frac{1}{2}\int_D \Phi^2 dl$, so that

$$r_S^2 \leq (\pi/2) r_c^2 \tag{2.15}$$

for all surfaces S.

We also introduce some definitions of the "radius" of S with respect to the unphysical flat geometry determined by the metric $\bar{h}_{ab}$. These measures of radius will be useful later in the proof of Theorems 1 and 2, and their various properties that we shall need are derived in Appendix A. The first measure is the "flat" Schwarzschild radius $\bar{r}_S$ defined by

$$\bar{r}_S = \sqrt{\frac{\bar{A}(S)}{4\pi}}, \tag{2.16}$$

where $\bar{A}(S)$ is the area computed in the flat geometry. This is to be distinguished from the physical Schwarzschild radius r_S introduced in Eq. (2.11). The capacity of S is [27]

$$r_0 = \frac{1}{4\pi}\oint_S \bar{n}^a \bar{D}_a \psi \; d^2\bar{S} \tag{2.17}$$

where ψ is the unique function satisfying $\bar{D}^a\bar{D}_a\psi = 0$ outside S, $\psi = -1$ on S, and $\psi \to 0$ at infinity. Finally we define the quantities

$$r_* = \frac{1}{8\pi}\oint_S p \; d^2\bar{S}, \tag{2.18}$$

where $p \equiv \bar{D}_a \bar{n}^a$ is twice the mean curvature of S, and

$$r_e = \frac{1}{4\pi}\oint_S (\kappa_g/\psi_n)\; d^2\bar{S}, \tag{2.19}$$

where κ_g is the Gauss curvature of S and $\psi_n \equiv \bar{n}^a\bar{D}_a\psi$. It is known [27] that

$$\bar{r}_S \leq r_* \tag{2.20}$$

and that

$$r_0 \leq r_*, \tag{2.21}$$

for all convex surfaces S.

B. Compact bodies cannot be static

We now turn to a proof of Theorem 1. Suppose that S is a level surface of Φ, so that $\Phi = A$ on S, where A is a constant. Suppose also (in accordance with the statement of Theorem 1) that S is convex with respect to the flat three-geometry. Then

$$r_c = A^2 \max\left[\rho_m, L(D)/\pi\right], \tag{2.22}$$

where $\rho_m = \max_{x\in D}\rho(x)$ and $L(D)$ is the length of the curve D. Also from Eqs. (2.9), (2.10), and (2.17) we have that $m_\infty = 2(A-1)r_0(S)$. This implies from the positive energy theorems that $A \geq 1$. Combining these yields that

$$\frac{m_\infty}{r_c} = f_1(A) f_2(S), \tag{2.23}$$

where $f_1(A) \equiv 4(A-1)/A^2$ which is bounded above by 1 for $A \geq 1$, and

$$f_2(S) \equiv \min\left\{\frac{r_0}{2\rho_m}, \frac{\pi r_0}{2L(D)}\right\}. \tag{2.24}$$

Now in Ref. [14], Sec. III C it is shown that, when S is convex, then

$$\frac{r_0}{L(D)} \leq \frac{1}{4}\sqrt{1+\pi^2/4}. \tag{2.25}$$

Thus we finally obtain

$$m_\infty / r_c \leq \alpha, \tag{2.26}$$

where $\alpha \equiv \pi(1+\pi^2/4)^{\frac{1}{2}}/8 \approx 0.73$. This completes the proof.

C. Outer trapped surfaces

In this section, we carry through the proof of Theorem 2, in stages. First of all, in Lemma 1, we show that if S is an averaged trapped surface, then $m_\infty / r_S(S) \gtrsim 1/\Phi_{|S}$. A similar lower bound is found in Lemma 2 for the ratio $m_\infty / r_c(S)$. Then in Lemma 3, we show that with certain assumptions the conformal factor Φ cannot be large on the outermost averaged trapped surface. Finally we combine these three lemmas with Eq. (2.38) to arrive at the theorem.

Suppose that S is an arbitrary surface in Σ_e which encloses the source. Let $\Phi_{\min}$ and $\Phi_{\max}$ be the minimum and maximum values of the conformal factor Φ on S. By combining Eqs. (2.7) and (2.10) one gets

$$m_\infty = \frac{1}{8\pi}\oint_S p\Phi \; d^2\bar{S} - \frac{1}{8\pi}\oint_S \theta_{\rm out}\Phi^3 \; d^2\bar{S}. \tag{2.27}$$

We will call S an averaged trapped surface if the last term on the right hand side above is positive. Note that this differs from the conventional definition of averaged trapped [4] in that the weighting factor is chosen to be Φ^3 instead of Φ^4. Now if S is convex with respect to $\bar{h}_{ab}$ so that the mean curvature $2p$ is positive, and if also S is averaged trapped, then from Eqs. (2.27) and (2.18) it follows that $m_\infty \geq \Phi_{\min} r_*$. Combining this with Eqs. (2.20), (2.11), and (2.16) proves the following.

Lemma 1. Let S be a closed surface enclosing the source region Σ_i which is convex with respect to $\bar{h}_{ab}$. If S is averaged trapped then

$$\frac{m_\infty}{r_S(S)} \geq \frac{\Phi_{\min}}{\Phi_{\max}^2}. \tag{2.28}$$

A similar result holds for the circumferential radius r_c. If we assume that S is a convex, axisymmetric, averaged trapped surface, then Eqs. (2.12)–(2.14) similarly yield that

$$\frac{m_\infty}{r_c} \geq \frac{\Phi_{\min}}{\Phi_{\max}^2}\, r_* \, \max\left(\frac{L(D)}{\pi}, \rho_m\right)^{-1}. \tag{2.29}$$

We claim that $r_* \geq L(D)/4$. To see this, suppose that the surface is defined by the equation $\rho = R(z)$, for $z_0 \leq z \leq z_1$. Then from Eq. (2.18),

$$r_* = \frac{1}{4}\int_D pR\,dl, \tag{2.30}$$

where $p = 1/(Rv) - R''/v^3$, $v^2 = 1 + R'^2$, and primes denote differentiation with respect to z. Now integrating by parts and using the inequality

$$1 + R'\arctan R' \;\geq\; \sqrt{1+R'^2}$$

proves the claim.

From Eq. (2.29) it is clear that we also need to find a lower bound for the quantity r_*/ρ_m. Using the fact that $L(D) \geq 2\rho_m$ (which is apparent from a diagram), we see that $r_*/\rho_m \geq 1/2$. In fact in Appendix A we show that this can be improved to $r_*/\rho_m \geq \pi/4$. Inserting these results into Eq. (2.29) gives the following lemma.

Lemma 2. Let S be a closed, axisymmetric surface enclosing the source region Σ_i, which is convex with respect to $\bar{h}_{ab}$. If S is averaged trapped then

$$\frac{m_\infty}{r_c(S)} \geq \frac{\pi}{4}\,\frac{\Phi_{\rm min}}{\Phi^2_{\rm max}}. \tag{2.31}$$

As the next step in our proof of Theorem 2, suppose that there is some outer-trapped, level surface S in the external region Σ_e. Then in particular there will be averaged trapped, level surfaces. For these surfaces, the lower bounds derived in Lemmas 1 and 2 will get better as Φ gets smaller. The optimum lower bound will occur at the outermost, level, averaged trapped surface, for which the average value of $\theta_{\rm out}$ vanishes. Such a surface will exist because Σ is asymptotically flat. We now show that the value of the conformal factor Φ on this particular surface (call it $S_{\rm outer}$) is bounded above.

Lemma 3. Let $\Phi_{\rm outer}$ be the value of Φ on the outermost, averaged trapped, level surface $S_{\rm outer}$. Then

$$1/\Phi_{\rm outer} \geq 1 - \sqrt{\frac{r_e}{2r_0}}. \tag{2.32}$$

Here r_e and r_0 are the radius functions introduced in Sec. II A, and are evaluated at $S_{\rm outer}$.

To derive this bound, suppose that S is a level surface of Φ. Then combining Eqs. (2.18), (2.27), and (A24) yields that

$$\frac{1}{8\pi m_\infty r_*(S)}\oint_S \Phi^3\theta_{\rm out}\,d^2\bar{S} = \frac{1}{m_\infty} + \frac{1}{2r_0(S)} - \frac{1}{r_*(S)}. \tag{2.33}$$

This provides us with a necessary and sufficient condition for S to be averaged trapped, namely, that the right-hand side above be negative. (For spherical spacetimes $r_0 = r_*$ and we recover the well known condition $m > 2r$.) Evaluating Eq. (2.33) at $S_{\rm outer}$ and using Eq. (A24), one finds that

$$r_*(S_{\rm outer}) = m_\infty/\Phi_{\rm outer}. \tag{2.34}$$

Now both sides of Eq. (2.33) can be considered as functions of the parameter r_0, which increases monotonically as one moves outward through the foliation of level surfaces (see Appendix A). If $r_{\rm crit} \equiv r_0(S_{\rm outer})$ and $\langle\theta_{\rm out}\rangle \equiv \oint \Phi^3\theta_{\rm out}\,d^2S$, then the equation can be written as

$$f(r_0)\,\langle\theta_{\rm out}\rangle\,(r_0) = g(r_0)$$

where f is a positive function. Since $S_{\rm outer}$ is the outermost averaged trapped surface, we must have $\langle\theta_{\rm out}\rangle\,(r_{\rm crit}) = 0$ and $\partial_{r_0}\langle\theta_{\rm out}\rangle\,(r_{\rm crit}) \geq 0$. This implies that $g'(r_{\rm crit}) \geq 0$, or

$$\frac{-1}{2r_0^2} + \frac{1}{r_*^2}\frac{\partial r_*}{\partial r_0} \geq 0. \tag{2.35}$$

Using Eqs. (2.34), (A24) and ($A25$) we can write this as

$$\frac{\Phi^2_{\rm outer}}{(\Phi_{\rm outer}-1)^2} \geq \frac{2r_0}{r_e}, \tag{2.36}$$

which establishes Lemma 3.

Now from Eq. (2.32) it is clear that we would like to show that $r_e \lesssim r_0$ always. Unfortunately we have not been able to prove this. However we have evaluated the ratio r_e/r_0 for prolate and oblate ellipsoids, and for level surfaces of the function

$$\Phi = 1 + \frac{m}{2r} + \alpha\left(\frac{m}{2r}\right)^{l+1} P_l(\cos\theta) \tag{2.37}$$

with $\alpha \ll 1$, to second order in α. In all cases we find that r_e/r_0 decreases away from unity as the surface becomes less spherical. See Appendix B for details. This leads us to conjecture that all surfaces S embedded in flat three-dimensional space probably do satisfy the property

$$r_e(S) \leq r_0(S). \tag{2.38}$$

For initial data sets with the property that all the level surfaces in the external region satisfy the property (2.38), by combining the three lemmas we deduce Theorem 2 as quoted in the introduction.

III. CONCLUSION

In this paper we have have found conditions for outer trapped surfaces *not* to be present in an initial data set. This work supports the conclusion of Shapiro and Teukolsky that the matter and gravitational field configurations on a particular time slice can become arbitrarily singular without the appearance of an apparent horizon. However, it is not clear that this tells one anything about cosmic censorship, as Wald has shown that there are non-spherically symmetric foliations of standard black-hole spacetimes with no apparent horizons on any of the time slices [30]. It would be useful to find out just when can a spacelike hypersurface fail to register the presence of an event horizon by an apparent horizon.

ACKNOWLEDGMENTS

The author would like to acknowledge the inspiration gained from reading the papers of Edward Malec, and also to thank him for helpful correspondence. Thanks are also due to Eric Poisson, Curt Cutler and Richard Price for some useful discussions, and especially to Kip Thorne for his encouragement and comments. This work was supported in part by NSF Grants Nos. AST-8817792 and AST-9114925.

APPENDIX A: MEASURES OF RADIUS IN FLAT SPACE

Several different definitions of radius are possible for a surface in flat, three-dimensional space. In Sec. II A we defined for a closed surface S the capacity $r_0(S)$ [Eq. (2.17)], the Schwarzschild radius $\bar{r}_S(S)$ [Eq. (2.16)], the quantity $r_*(S)$ [Eq. (2.18)], and the quantity $r_e(S)$ [Eq. (2.19)]. The properties of these measures and the relationships between them form a crucial underpinning to our analysis of trapped surfaces. In this appendix we derive some of the properties which are quoted and used in the body of the paper.

It turns out that, in the derivation of these properties, it is useful not to consider a single closed surface S, but instead a foliation of surfaces. Accordingly, let S_0 be a two-surface with the topology of a sphere, and fix a foliation by similar surfaces of the region outside S_0. Then we can find coordinates σ, x^A ($A = 1, 2$) such that (i) the line element of the flat three-geometry takes the form

$$ds^2 = e^{2F(\sigma,x^A)}d\sigma^2 + h_{BC}(\sigma, x^A)dx^B dx^C, \quad \text{(A1)}$$

and (ii) the surfaces of the foliation are the surfaces of constant σ, such that σ increases monotonically as one moves outwards towards infinity. The extrinsic curvature tensor of a typical surface S_σ is given by

$$K_{AB} = \frac{1}{2}e^{-F}\dot{h}_{AB}, \quad \text{(A2)}$$

where the dot denotes differentiation with respect to σ. Its trace (twice the mean curvature of S) is

$$p = \frac{1}{2}e^{-F}h^{AB}\,\dot{h}_{AB}, \quad \text{(A3)}$$

which appears in the definition of the radius function $r_*(S)$. The Gauss curvature is the product of the eigenvalues of K_{AB} with respect to h_{AB}, which is

$$\begin{aligned}\kappa_g &= \frac{1}{2}\left[(\text{tr}K)^2 - \text{tr}K^2\right] \\ &= \frac{1}{8}e^{-2F}\left[(h^{AB}\dot{h}_{AB})^2 - \dot{h}_{AB}\dot{h}_{CD}h^{AC}h^{BD}\right]. \end{aligned}\quad \text{(A4)}$$

Now we make use of the fact that the three-geometry is flat. The Riemann tensor computed from the metric (A1) has components

$$\begin{aligned}R_{\sigma A\sigma B} &= \frac{1}{4}\left\{\dot{h}_A^{\ C}\dot{h}_{CB} + 2\dot{F}\dot{h}_{AB} - 2\ddot{h}_{AB}\right\} \\ &\quad -e^F\nabla_A\nabla_B e^F,\end{aligned}\quad \text{(A5)}$$

$$R_{\sigma ABC} = e^F\nabla_{[C}e^{-F}\dot{h}_{B]A}, \quad \text{(A6)}$$

$$R_{ABCD} = {}^{(2)}R_{ABCD} - \frac{1}{2}e^{-2F}\dot{h}_{A[C}\dot{h}_{D]B} \quad \text{(A7)}$$

Here ∇_A denotes the covariant derivative associated with the two-metric h_{AB}, the two-dimensional Riemann tensor of S_σ is ${}^{(2)}R_{ABCD}$, and $\dot{h}_{AB}$, $\ddot{h}_{AB}$, and F are regarded as tensor fields on S_σ. By equating these Riemann tensor components to zero, we obtain necessary and sufficient conditions for the functions F and h_{AB} to describe foliations of flat space. Since in two dimensions there is only one independent component of the Riemann tensor, these conditions are

$${}^{(2)}R = 2\kappa_g, \quad \text{(A8)}$$

$$\dot{h}_A^{\ C}\dot{h}_{CB} + 2\dot{F}\dot{h}_{AB} - 2\ddot{h}_{AB} = 4e^F\nabla_A\nabla_B e^F, \quad \text{(A9)}$$

and

$$\nabla_{[A}e^{-F}\dot{h}_{B]C} = 0. \quad \text{(A10)}$$

Next we derive a useful formula for the rate of change with respect to σ of the integral of any function over the surface S_σ. Using the fact that the area element of the surface is

$$d^2S = \sqrt{\det h_{AB}}\,dx^1dx^2,$$

we get

$$\begin{aligned}\partial_\sigma \oint_{S_\sigma} f\,d^2S &= \oint_{S_\sigma}(\partial_\sigma f + f\partial_\sigma \ln\sqrt{\det h_{AB}})\,d^2S \\ &= \oint_{S_\sigma}(\partial_\sigma f + e^F pf)\,d^2S.\end{aligned}\quad \text{(A11)}$$

The second equality here follows from Eq. (A3). In these equations and throughout this appendix, the symbol d^2S means the surface area element with respect to the flat background geometry, which was denoted $d^2\bar{S}$ in the body of the paper.

The radius functions $\bar{r}_S$, r_*, and r_0 are defined in Eqs. (2.16), (2.18), and (2.17). Evaluated on the surfaces S_σ these produce functions $\bar{r}_S(\sigma)$, $r_*(\sigma)$ etc. Using the formula (A11) we can find how these functions vary through the foliation. We find that

$$\partial_\sigma \bar{r}_S^2 = \frac{1}{4\pi}\oint e^F p\,d^2S \quad \text{(A12)}$$

and

$$\partial_\sigma r_* = \frac{1}{8\pi}\oint(\dot{p} + e^F p^2)\,d^2S. \quad \text{(A13)}$$

Now using Eqs. (A3), (A4), and (A9) after some manipulation we obtain

$$\dot{p} + e^F p^2 = 2e^F\kappa_g - \nabla^2 e^F, \quad \text{(A14)}$$

which when inserted in Eq. (A13) gives [26]

$$\partial_\sigma r_* = \frac{1}{4\pi}\oint e^F\kappa_g\,d^2S. \quad \text{(A15)}$$

To calculate $\partial_\sigma r_0$ is a little more complicated. Let $\psi_{(\tau)}(\sigma, x^A)$ be that harmonic function which takes the value -1 on S_τ and which vanishes at infinity. Then, from Eq. (2.17),

$$r_0(\sigma) = \frac{1}{4\pi}\left[\oint e^{-F}\partial_\sigma\psi_{(\tau)}\,d^2S\right]_{\tau=\sigma}, \quad \text{(A16)}$$

since $e^{-F}\partial_\sigma = \partial_n$ is the unit outward normal derivative. Now using Eq. (A11) gives

$$\dot r_0(\sigma) = \frac{1}{4\pi}\oint [\,\partial_\sigma\partial_n\psi_{(\tau)} + \partial_\tau\partial_n\psi_{(\tau)} + e^F p\,\partial_n\psi_{(\tau)}]\,d^2S\,\big|_{\tau=\sigma}. \tag{A17}$$

From the equation $D_a D^a\psi = 0$ and using the metric (A1) we find that

$$\partial_\sigma(e^{-F}\dot\psi) = -\dot\psi p - \nabla_A(e^F\nabla^A\psi). \tag{A18}$$

When this expression for $\partial_\sigma\partial_n\psi_{(\tau)}$ is inserted above, the second term is a total derivative which vanishes when integrated, and the first term cancels with the last term in Eq. (A17), so we get

$$\dot r_o(\sigma) = \frac{1}{4\pi}\left[\oint \partial_\tau\partial_n\psi_{(\tau)}\,d^2S\right]_{\tau=\sigma}. \tag{A19}$$

To evaluate this we find an approximate expression for $\psi_{(\tau)}$. Let $\tau = \sigma_0 + \varepsilon$, and suppose that $\psi_{(\tau)} = \psi_{(\sigma_0)} + \varepsilon f + O(\varepsilon^2)$. Then by demanding that $\psi_{(\tau)} = -1 + O(\varepsilon^2)$ on S_τ, we find that the function f is determined by the requirements $f(\sigma_0, x^A) = -\dot\psi(\sigma_0, x^A)$, $D^a D_a f = 0$, and $f \to 0$ at infinity. Also it follows that

$$\partial_\tau\psi_{(\tau)}(\sigma, x^A)\big|_{\tau=\sigma_0} = f(\sigma, x^A), \tag{A20}$$

and so from Eq. (A19), $\dot r_0 = \oint \partial_n f\,d^2S/4\pi$. Now by using Green's theorem $\oint \psi\partial_n f = \oint f\partial_n\psi$ we finally get

$$\dot r_0(\sigma) = \frac{1}{4\pi}\oint_{S_\sigma} e^{-F}\dot\psi^2_{(\sigma)}\,d^2S, \tag{A21}$$

where $\dot\psi_{(\sigma)} \equiv \partial_\sigma\psi_{(\tau)}(\sigma, x^A)\big|_{\tau=\sigma}$.

The rate of change Eqs. (A12), (A15), and (A21), together with the freedom to choose a particular foliation of surfaces S_σ starting from a given surface S_0, comprise powerful tools for deriving properties of the radius functions. By using these equations specialized to the foliation in which $F = 0$, Szego [27] shows that $\bar r_s \le r_*$ and $r_0 \le r_*$ always. It might be possible, using these tools, to prove the conjecture in Sec. II C [Eq. (2.38) above], although we have not been able to do so.

The results we need for this paper can be obtained by choosing the foliation to be the set of level surfaces of a harmonic function. In the notation introduced above, let S_0 be a given initial surface corresponding to $\sigma = \sigma_0$, put $\chi = \psi_{(\sigma_0)}$, and choose the foliation to be the level surfaces of χ. It follows that $\chi = \chi(\sigma)$, i.e., that χ is independent of the coordinates x^A, and also that

$$\psi_{(\tau)} = -\chi/\chi(\tau). \tag{A22}$$

Now using Eqs. (2.17), (A21), (A22), and the fact that $\partial_n\psi_{(\tau)} = -e^{-F}\dot\chi/\chi(\tau)$, we get

$$\dot r_0(\sigma) = -\frac{\dot\chi(\sigma)}{\chi(\sigma)} r_0(\sigma). \tag{A23}$$

This means that χ must be of the form $\chi(\sigma) = A + B/r_0(\sigma)$ for some constants A and B. The conformal factor Φ of this paper clearly must also be of this form, and from Eq. (2.10) and the boundary condition at infinity it follows that

$$\Phi(\sigma) = 1 + \frac{m_\infty}{2r_0(\sigma)}, \tag{A24}$$

which is one of the results used in Sec. II C.

Next, if we combine Eqs. (A15), (2.19), and (A23) we find that $\dot r_* = \dot r_0 r_e/r_0$. Hence if we consider r_* as a function of r_0 instead of σ [r_0 increases monotonically with σ, cf. Eq. (A21)], then we get

$$\frac{\partial r_*}{\partial r_0} = \frac{r_e}{r_0}. \tag{A25}$$

This is the quantity that we conjecture to be always less than 1, and that we use in the derivation of Lemma 3.

The final result concerns a convex axisymmetric surface S, defined by an equation of the form $\rho = R(z)$ for $z_0 \le z \le z_1$. Here (z, ρ, φ) are standard cylindrical coordinates, and $R(z_0) = R(z_1) = 0$. In Sec. II C we claimed that $r_*(S) \ge (\pi/4)\rho_m$ always, where $\rho_m \equiv \max_z R(z)$. This can be derived by means of the following trick. We can find a surface S' inside S which is a pancake shaped ellipsoid of revolution, of the form

$$\frac{(z-\bar z)^2}{z_m^2} + \frac{\rho^2}{\rho_m^2} = 1,$$

where $\bar z$ is such that $R(\bar z) = \rho_m$, and we choose z_m to be small enough so that S' fits inside S. Now clearly we can find a foliation of convex surfaces interpolating between S' and S. Hence by Eq. (A15) we see that

$$r_*(S) \ge r_*(S'). \tag{A26}$$

But a straightforward calculation gives that, in the limit where $z_m \to 0$, $r_*(S') = \pi\rho_m/4$ [cf. Eq. (B15) below]. This proves the claim.

APPENDIX B: THE CONJECTURE $r_e \le r_0$

In this Appendix we calculate the ratio r_e/r_0 for several classes of surfaces using the formalism described in Appendix A. Consider firstly prolate ellipsoids. The appropriate form of the metric (A1) describing flat space is

$$ds^2 = a^2(\sinh^2 u + \sin^2 v)(du^2 + dv^2) + a^2\sinh^2 u\sin^2 v\,d\varphi^2 \tag{B1}$$

where the $u =$ constant surfaces surfaces are prolate ellipsoids of eccentricity $\varepsilon = \operatorname{sech} u$. If we define

$$\chi = -\ln\tanh(u/2) \tag{B2}$$

and $\Delta^2 = \sinh^2 u + \sin^2 v$, we find from Eqs. (A3) and (A4) that

$$p = \frac{2\sinh^2 u + 1 - \cos^2 v}{a\Delta^3\tanh u} \tag{B3}$$

and

$$\kappa_g = \frac{\cosh^2 u}{a^2\Delta^4}. \tag{B4}$$

Also since χ is harmonic, $\psi_n = -e^{-F}\dot{\chi}/\chi$, and it follows that

$$\psi_n = [a\chi\Delta \sinh u]^{-1}. \tag{B5}$$

Using the definitions of the radius functions, we calculate that

$$r_0 = a/\chi, \tag{B6}$$

$$r_* = \frac{1}{2} a \cosh u \left[1 + \chi \sinh u \tanh u\right], \tag{B7}$$

and

$$r_e = a\chi^2 \cosh u \sinh^2 u. \tag{B8}$$

The ratio r_e/r_0 is plotted as a function of the eccentricity $\varepsilon = \text{sech}u$ in Fig. 2 (lower curve); it is always smaller than unity.

For oblate ellipsoids the discussion is exactly analogous so we merely list the equations:

$$ds^2 = a^2(\sinh^2 u + \sin^2 v)(du^2 + dv^2) + a^2 \cosh^2 u \cos^2 v \, d\varphi^2, \tag{B9}$$

$$\chi = 2 \, \text{arctan} e^{-u}, \tag{B10}$$

$$p = \frac{2\sinh^2 u + 1 + \sin^2 v}{a\Delta^3 \coth u}, \tag{B11}$$

$$\kappa_g = \frac{\sinh^2 u}{a^2 \Delta^4}, \tag{B12}$$

$$\psi_n = [a\chi\Delta \cosh u]^{-1}, \tag{B13}$$

$$r_0 = a/\chi, \tag{B14}$$

$$r_* = \frac{1}{2} a \sinh u \left[1 + \chi \cosh u \coth u\right], \tag{B15}$$

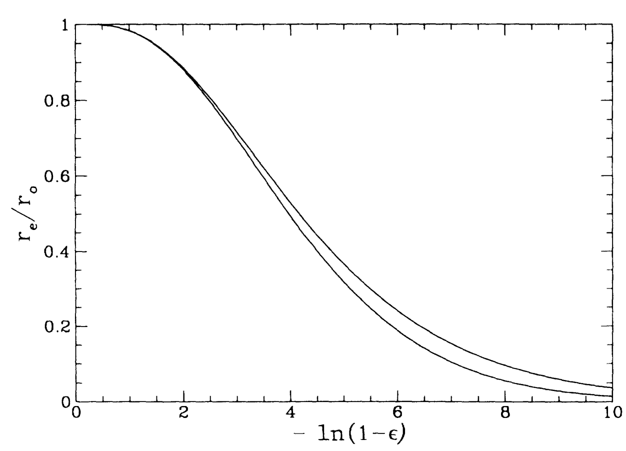

FIG. 2. The ratio r_e/r_0 plotted as a function of eccentricity ε for prolate (lower curve) and oblate (upper curve) ellipsoids. Notice that it decreases away from unity as the surfaces become less spherical.

$$r_e = a\chi^2 \cosh^2 u \sinh u; \tag{B16}$$

see the upper curve in Fig. 2.

Finally consider level surfaces of the function

$$\Phi = 1 + \frac{m}{2r} + \alpha \left(\frac{m}{2r}\right)^{l+1} P_l(\cos\theta), \tag{B17}$$

where $\alpha \ll 1$, P_l is the lth Legendre polynomial, and (r, θ, φ) are standard spherical polar coordinates. A straightforward calculation shows that, for the surface $\Phi = A$,

$$\frac{r_e}{r_0} = 1 - c_l \alpha^2 + O(\alpha^3), \tag{B18}$$

where $c_l = (A-1)^{2l} 2l^2(2l-1)/(2l+1)$. The ratio decreases away from unity as α is increased for all values of l.

We remark that our conjecture $r_e \leq r_0$ is similar to a conjecture of Malec [Eq. (16) of Ref. [19]], which in our notation reads $r_e r_0 \leq r_*^2$. By Eq. (2.21), this would be a consequence of $r_e \leq r_0$. Also it is known that the corresponding pointwise inequality $\kappa_g \leq \psi_n^2$ is not always true.

APPENDIX C: THIN ELLIPSOIDAL SHELLS

In this appendix we examine a class of initial data sets which contain momentarily static, ellipsoidal, thin shells of matter. The distribution of surface matter density that we assume is nonuniform, but is chosen to make the calculations simple. We analytically determine when and where outer trapped and averaged outer trapped level surfaces occur in these data sets, and calculate the ratios m_∞/r_c and m_∞/r_S. The conclusions are that (i) the qualitative behavior of the ratio m_∞/r_c is in accordance with Fig. 1, and (ii) whenever outer trapped level surfaces occur, the quantity $\Theta_{\max} \equiv \max_S m_\infty/r_c(S)$ is larger than some critical value Θ_c. For prolate initial data sets $\Theta_c = 0.4889$, and for oblate ones $\Theta_c = 0.4799$.

A closely related class of initial data sets was examined by Nakamura, Shapiro and Teukolsky in Ref. [15], where they numerically calculated $\Theta_{\max}$ for various matter configurations, and related its value to the presence of apparent horizons. Here we obtain similar results by analytic methods.

To describe the results in more detail we now discuss the parameters used to describe the shell. A shell will be determined by (i) the semimajor axis α of the ellipse that generates the ellipsoid by a rotation, (ii) the eccentricity ε of this ellipse, and (iii) the proper mass m_p of the shell. This is defined as

$$m_p = \int \rho_M \, d^3V = \int \rho_M \Phi^6 \, d^3\bar{V}. \tag{C1}$$

Now sometimes two different shells will give rise to the same external three-geometry [28]. This will be the case if the values for each shell of the following two combinations of the above parameters are the same:

$$m_\infty = m_p \left[1 - \frac{m_p}{2\alpha}\frac{\chi(\varepsilon)}{\varepsilon}\right], \tag{C2}$$

and

$$\Gamma = \left[\frac{2\alpha\varepsilon}{m_p} - \chi(\varepsilon)\right]^{-1}. \tag{C3}$$

Here $\chi = \ln\left[(1+\varepsilon)/(1-\varepsilon)\right]/2$ in the prolate case, and $\chi = 2\arctan\left[(1-\sqrt{1-\varepsilon^2})/\varepsilon\right]$ in the oblate case. The dimensionless parameter Γ^2 is essentially the ratio of the asymptotic mass of the shell cubed to its quadrupole moment, and m_∞ is the asymptotic mass [29].

We also introduce a dimensionless radial coordinate u (see below) with the properties that (i) the shell is the surface $u = u_0$, with $\varepsilon = \operatorname{sech} u_0$, (ii) the level surfaces of the conformal factor Φ and of u coincide, and (iii) u increases monotonically as one goes outwards from the shell towards infinity. The parameters Γ, m_∞, and u_0 turn out to be a more convenient set to use to describe the shell than α, ε, and m_p. Now any level surface in any of these data sets may be specified by giving values of u and Γ, since it does not matter at which $u_0 < u$ the shell is located, and without loss of generality we can take $m_\infty = 1$.

The results we obtain [Eqs. (C6), (C8), (C12), and (C14) below] are summarized graphically in Figs. 3 and 4, which are diagrams of this parameter space of level surfaces. They show where outer trapped and averaged outer trapped level surfaces occur, and where the ratios m_∞/r_c and m_∞/r_S have local maxima or minima. These ratios as a function of u along the line $\mathcal{AB}$ in Fig. 3 are shown in Fig. 5. We see that at shells such as that corresponding to the point $\mathcal{P}$ in Fig. 3 the ratio m_∞/r_S

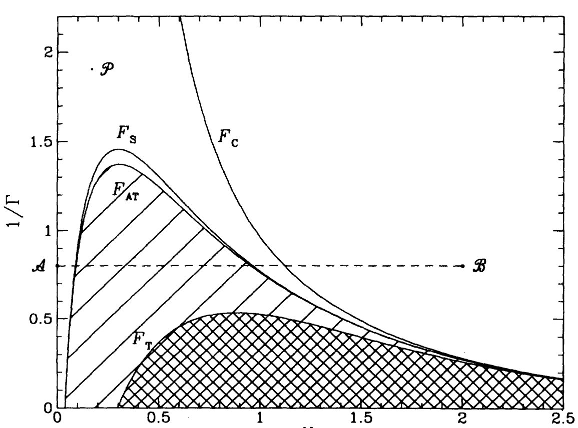

FIG. 3. The behavior of prolate initial data sets. Each point $(u_0, 1/\Gamma)$ in this diagram corresponds to a shell, and all the points $(u, 1/\Gamma)$ with $u \geq u_0$ correspond to the level surfaces in the three-geometry outside the shell. (The value of u_0 can be anything one wishes and thus is not shown explicitly here.) The hatched region contains outer trapped surfaces, and the region shaded by lines contains averaged outer trapped surfaces. The curves F_C and F_S show where the level surfaces of minimum circumference and of extremal area occur.

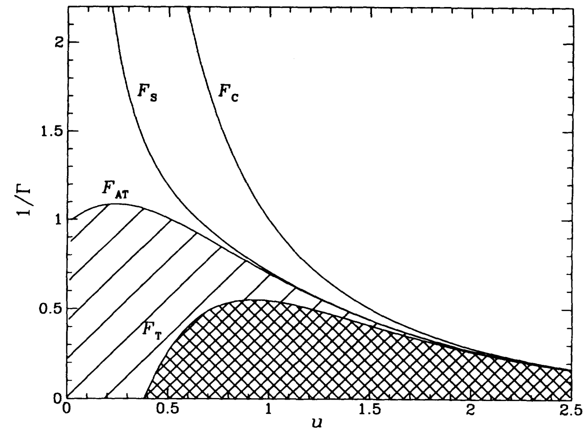

FIG. 4. A similar diagram for oblate initial data sets.

can be arbitrarily large, even though there are no trapped level surfaces or averaged trapped level surfaces anywhere outside these shells. This shows that area is not as useful a measure of size as circumference, at least for prolate geometries. Notice that the behavior of m_∞/r_S is quite different in the oblate case.

Also we see that if one imagines traveling inwards from infinity in an initial data set, one encounters first the level surface of minimum circumference, then the one of minimum area, then the outermost, outer averaged trapped level surface, and finally the outermost outer trapped level surface. These all coincide in the limit $\Gamma \to \infty$, i.e., in the limit of spherical symmetry. In the prolate case, the plot suggests (but does not prove) that there is an antitrapped region at small u values containing no averaged outer trapped surfaces, such as is found inside the inner horizon of a Reissner-Nordström black hole.

It is also apparent that outer trapped level surfaces are present if and only if Γ is greater than some critical

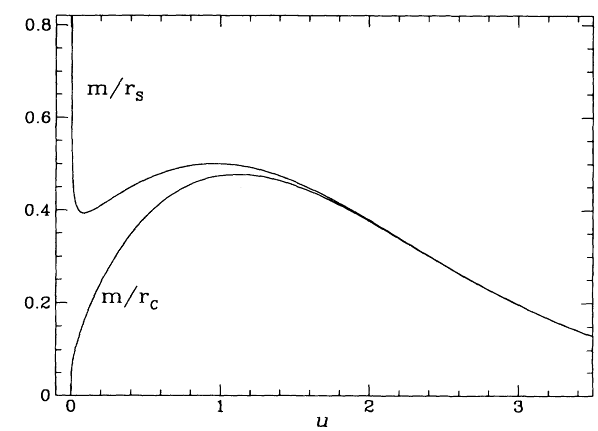

FIG. 5. The shape of the functions $m_\infty/r_c(u,\Gamma)$ and $m_\infty/r_S(u,\Gamma)$ can be visualized easily be combining this figure with Fig. 3. This plot shows how these quantities vary with u in the prolate case when $\Gamma = 1.25$, i.e., along the line $\mathcal{AB}$ above.

value Γ_c, where $\Gamma_c = 1.876$ (prolate case), or $\Gamma_c = 1.819$ (oblate case). The quantity $\max_u m_\infty / r_c(u)$ can be calculated numerically and increases monotonically with Γ, asymptoting to the value of 1/2. Therefore outer trapped level surfaces are present only when $\max_u m_\infty/r_c(u)$ is large enough, in accordance with Theorem 2.

We now turn to a derivation of these results. The starting point is the line element (2.8), where the base metric $\bar{h}_{ab}$ is described in coordinates (u, v, φ) according to Eq. (B1) [Eq. (B9) in the oblate case]. The conformal factor we use is

$$\Phi = \begin{cases} 1 + \Gamma\chi(u), & u \geq u_0, \\ 1 + \Gamma\chi(u_0), & u < u_0, \end{cases} \tag{C4}$$

where χ is the harmonic function defined in Eq. (B2) [Eq. (B10)]. From the Lichnerowicz equation (2.3) it is apparent that this describes a thin shell of matter, with surface density proportional to $e^{-2F} = 1/\Delta^2$. Using Eqs. (A24), (C4), (B6), and (B14), we find that $m_\infty = 2\Gamma a$. But from Eqs. (C1) and (2.10) we obtain

$$m_\infty = \frac{m_p}{\Phi(u_0)}. \tag{C5}$$

Equations (C2) and (C3) can be derived from this, using also that $\alpha = \Phi(u_0)^2 a \cosh u_0$ and $\varepsilon = \operatorname{sech} u_0$.

Consider now a level surface S_u which is in the external region, so that $u \geq u_0$. From Eqs. (2.33) and (A24) we see that it will be averaged trapped iff $1/\Phi_{|S} \leq 1 - r_*/(2r_0)$. By Eq. (C4) this occurs if and only if $1/\Gamma \leq F_{\rm AT}(u)$, where

$$F_{\rm AT}(u) = \chi(u)(2r_0/r_* - 1). \tag{C6}$$

This function was evaluated using the expressions for χ, r_0 and r_* in Appendix B to produce the plots in Figs. 3 and 4. It is similarly straightforward to find when will the surface S_u be pointwise outer trapped. From Eq. (2.7) with $\bar{K}_{ab} = 0$, we find that

$$\Phi^2\theta_{\rm out} = p + \frac{4}{\Phi}\partial_n\Phi.$$

But if $A \equiv \Phi_{|S}$ and $\psi \equiv \psi_{(u)}$ in the notation of Appendix A, then $\Phi = 1 + (1 - A)\psi$, and so $A^2\theta_{\rm out} = p - 4(1 - 1/A)\psi_n$. Hence S_u will be outer trapped if and only if

$$1 - \frac{1}{\Phi_{|S}} \geq \max_S \frac{p}{4\psi_n}, \tag{C7}$$

which from Eq. (C4) is equivalent to $1/\Gamma \leq F_T(u)$, where

$$F_T(u) = \chi(u)\left[\min_S \frac{4\psi_n}{p} - 1\right]. \tag{C8}$$

Using Eqs. (B2), (B3), (B5), etc. we find that

$$F_T(u) = \begin{cases} 2\operatorname{sech} u + \ln[\tanh u/2] & \text{prolate case,} \\ \frac{4\sinh u}{1+2\sinh^2 u} - 2\ \operatorname{arctan} e^{-u} & \text{oblate case.} \end{cases} \tag{C9}$$

Next we find where the surfaces of extremal area occur. Now the physical Schwarzschild radius r_S is related to the flat space Schwarzschild radius $\bar{r}_s$ by $r_S = \Phi^2\bar{r}_s$. Also from the metrics (B1) and (B9), it follows that

$$\bar{r}_S^2 = \frac{1}{2}a^2\sinh^2 u\,[1 + \cosh u \coth u\ \arcsin(\operatorname{sech} u)] \tag{C10}$$

in the prolate case, and

$$\bar{r}_S^2 = \frac{1}{2}a^2\cosh^2 u\,[1 + \sinh u \tanh u\ \operatorname{arcsinh}(\operatorname{csch} u)] \tag{C11}$$

in the oblate case. If S_u is a surface of extremal area, then $\dot{r}_S = 0$, i.e., $2\dot{\Phi}\bar{r}_S + \Phi\dot{\bar{r}}_S = 0$. From Eq. (C4), this is equivalent to $1/\Gamma = F_S(u)$, where

$$F_S = -\chi - \dot{\chi}\bar{r}_S/\dot{\bar{r}}_S. \tag{C12}$$

A similar method can be used to find the surfaces of minimum circumference. If we define the quantity $\bar{r}_c = \Phi^{-2}r_c$, then we find that

$$\bar{r}_c = \begin{cases} \frac{2a}{\pi}\cosh u\, E(\operatorname{sech}^2 u) & \text{prolate case} \\ a\cosh u & \text{oblate case.} \end{cases} \tag{C13}$$

Then the function

$$F_C = -\chi - \dot{\chi}\bar{r}_c/\dot{\bar{r}}_c. \tag{C14}$$

satisfies $F_C(u) = 1/\Gamma$ when $\dot{r}_c(u) = 0$. These equations determine the functions F_C and F_S which are plotted in Figs. 3 and 4.

Finally the ratio $\Theta = m_\infty/r_c$ is given by

$$\Theta = \frac{2\Gamma a}{[1 + \Gamma\chi(u)]^2\,\bar{r}_c(u)}. \tag{C15}$$

Evaluating this along the curves F_C in Figs. 3 and 4 produces in each case a function of Γ, $\Theta_{\rm max}(\Gamma)$, which turns out to be monotonically increasing. Evaluated at the critical value Γ_c below which there are no trapped level surfaces yields the value $\Theta_{\rm max}(\Gamma_c) = 0.4889$ in the prolate case, and $\Theta_{\rm max}(\Gamma_c) = 0.4799$ in the oblate case. Outer trapped level surfaces will be present only when $\Theta_{\rm max}$ is greater than these critical values.

[1] R. Penrose, Ann. N.Y. Acad. Sci. **224**, 125 (1973).
[2] R. Wald, *General Relativity* (University of Chicago Press, Chicago, 1984), p. 310.
[3] W. Israel, Can. J. Phys. **64**, 120 (1986).
[4] J.B. Hartle and D.C. Wilkins, Phys. Rev. Lett. **31**, 60 (1973).
[5] P.N. Demmie and A.I. Janis, J. Math. Phys. **14**, 793 (1973).
[6] R. Schoen and S.T. Yau, Commun. Math. Phys. **90**, 575 (1983).
[7] P. Bizon, E. Malec, and N. O'Murchadha, Phys. Rev. Lett. **61**, 1147 (1988).
[8] R. Arnowitt, S. Deser, and C.W. Misner, in *Gravitation: An Introduction to Current Research*, edited by L. Witten

(Wiley, New York, 1962).

[9] By proper mass we mean the integral over a region in a spacelike hypersurface of the stress energy tensor doubly contracted with the normal to that hypersurface.

[10] For an example of this effect, see N. O'Murchadha, Class. Quantum. Grav. **7**, 1953 (1990), Eq. (1.18) in the limit where $M \rightarrow 2L$.

[11] This has come about largely through a series of papers by Bizon, Malec, and O'Murchadha. See Malec [17] for a review.

[12] See Bizon, Malec, and O'Murchadha [7]. The conditions involving the proper mass m_p also require the assumption that the unique conformally flat spacelike hypersurface containing S be momentarily static, and the proper mass is defined using this hypersurface.

[13] K.S. Thorne, in *Magic Without Magic: John Archibald Wheeler*, edited by J. Klauder (Freeman, San Francisco, 1972), p. 231.

[14] E. Flanagan, Phys. Rev. D **44**, 2409 (1991).

[15] T. Nakamura, S.L. Shapiro, and S.A. Teukolsky, Phys. Rev. D **38**, 2972 (1988).

[16] S.L. Shapiro and S.A. Teukolsky, Phys. Rev. Lett. **66**, 994 (1991); Am. Scientist **79**, 330 (1991).

[17] E. Malec, Acta Phys. Pol. B **22**, 829 (1991).

[18] C. Barrabes, W. Israel, and P.S. Letelier, Phys. Lett. A **160**, 41 (1991); **161**, 562(E) (1992).

[19] E. Malec, Phys. Rev. Lett. **67**, 949 (1991). See also Malec [17] for a comprehensive review of this and related work.

[20] J.A. Wheeler, in *Relativity, Groups, and Topology*, edited by Bryce DeWitt and Cecile DeWitt (Gordon and Breach, New York, 1964).

[21] C.W. Misner, K.S. Thorne, and J.A. Wheeler, *Gravitation* (Freeman, San Francisco, 1973), p. 515.

[22] J. York, in *Gravitational Radiation*, edited by T. Piran and N. Deruelle (North-Holland, Amsterdam, 1982).

[23] N. O'Murchadha, in *Proceedings of the Center for Mathematical Analysis*, edited by R. Bartnick (Australian National University, Canberra, 1989), Vol. 19, p. 137. See also Wald, *General Relativity* [2] for a proof that outer trapped surfaces must lie inside event horizons in asymptotically predictable spacetimes (modulo a topological condition which is satisfied in the case considered in this paper).

[24] This will be the case if Σ_i is large enough to include all the points at which the gradient of Φ vanishes; see Flanagan [14].

[25] In fact it is only necessary to assume that the extrinsic curvature tensor K_{ab} is a pure trace, then the rest of our assumptions imply that it must vanish in the external region. The author is grateful to J. Eisenberg for bringing up this point.

[26] This formula was previously established using a different method by E. Malec, Acta. Phys. Pol. B **22**, 347 (1991).

[27] G. Szego and G. Polya, Am. J. Math. **67**, 1 (1945).

[28] In the sense that the region external to one shell will be iosmetric to a submanifold of the region external to another one.

[29] Notice that the negative, gravitational potential energy term in m_∞ increases with increasing eccentricity.

[30] R. Wald and V. Iyer, Phys. Rev. D **44**, 3719 (1992).